EFFECT OF LOUVER ANGLE ON PERFORMANCE OF PARALLEL FLOW HEAT EXCHANGER

by

Fengye YANG[a*], Pengfei ZHAO[b], Haijun LI[a], Jingkang KOU[a], Junjie ZHAI[a], and Xiuqing WU[a]

[a] School of Energy and Environment, Zhongyuan University of Technology, Zhengzhou, Henan, China
[b] Henan Electric Power Transmission and Transformation Construction Co., Ltd., Zhengzhou, Henan, China

Original scientific paper
https://doi.org/10.2298/TSCI2303907Y

In order to study the influence of the louver angle on the heat transfer and flow resistance characteristics of a parallel flow heat exchanger, this paper establishes five calculation models including a uniform angle model and four variable angle models for comparing and analyzing the temperature, velocity, and pressure fields, and evaluates their comprehensive performance. The results show that the suitable choice of the v louver angle can lead to an optimal heat transfer effect and a best comprehensive performance.

Key words: *louver angle, numerical simulation, comprehensive performance*

Introduction

Since the middle of last century, louver fins have been widely used in automobile air conditioning because of their small size, compact structure and various forms. The structure of louver fin not only increases the disturbance of fluid in the flow channel, but also changes the direction of fluid-flow, so as to enhance heat transfer and to improve heat transfer efficiency. Therefore, the study of louver fins is also favored by researchers.

In addition to the fin length, the fin spacing and the louver spacing, the louver angle also affects the heat transfer performance. There was much literature on the structure of louver fins with different angles. Beamer and Cowell [1] first proposed the structure of variable-angle louver fin, and found that although the variable-angle fin can cause pressure drop, the heat transfer performance has been improved much. Hsieh and Jang [2] studied four fin structures with different angles by means of numerical simulation, and concluded that the heat transfer of fin structures with variable angles was greatly improved compared with that of fin structures with fixed angles. Zhou *et al.* [3] conducted simulation studies on four groups of different shutter angles, and concluded that 24° was the optimal shutter angle, and the pressure loss increased as the fin angle increased. Zhou *et al.* [4] and Yan and Zhou [5] further studied the angle of the louver, the results showed that the heat transfer and pressure drop increased with the increase of window opening angle. Li *et al.* [6] found that the heat transfer coefficient increased first and then decreased with the increase of the angle. When the shutter angle is 24°, the heat exchanger has the best effect. The previous study results show that the heat transfer ef-

* Corresponding author, e-mail: 15981890068@126.com

fect of the heat exchanger can be improved by properly setting the angle of the shutter fin angle reasonably. Guo *et al.* [7] proposed eight kinds of variable angle fin structures, and analyzed their advantages and disadvantages, the results showed that the heat transfer capability of the eight models is improved, and the overall performance is the best when the attack angle gradient is 1.2°.

In recent years, there was little research on the angle of louver, therefore, based on a conventional uniform angle fin structure, four new types of variable angle fin structures are proposed for 3-D numerical analysis, the heat transfer performance of five sets of louvers with different angles is analyzed.

Model and boundary condition

Physical model

In this paper, five groups of fin models are established. Their simplified structures and initial parameters are shown in fig. 1 and tab. 1, respectively. According to the present study on a uniform angle louver fin structure D is selected, four variable angle fin structures A, B, C, and E are shown in fig. 2.

Table 1. Initial parameters of the model

Parameter name	Parameter value	Parameter name	Parameter value
Louver space L_P [mm]	1	Louver thickness δ [mm]	0.1
Louver length L_L [mm]	6.8	Inlet louver length L_1 [mm]	1.5
Louver height F_L [mm]	7.4	Turn area length L_2 [mm]	2.0
Fin length F_d [mm]	14.95	Outlet louver length L_3 [mm]	1.5

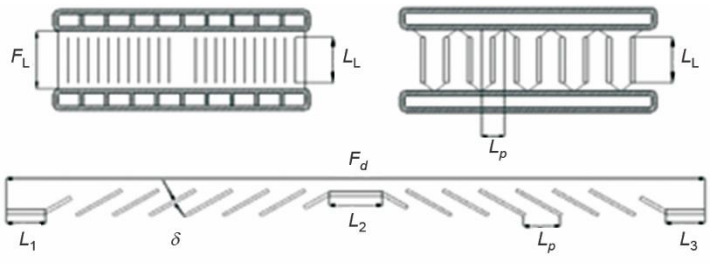

Figure 1. The basic structure of louver fins

Because of the periodicity and complexity of the louver fins, only one row of the louver fins is selected for simulation in this paper. Figure 3 shows the 3-D structure of the louver fins, in which the fluid region is the fluid flow region, and the solid region contains eight louver fins and flat tube walls, so it is an aeroelastic system [8].

Governing equation

The numerical simulation is a powerful tool to the study of various complex problems, for examples, the gas journal bearing system [9] and the peristaltic flow [10]. The numerical approximation always depends upon an effective iteration algorithm [11-13]. This pa-

per adopts 3-D incompressible and laminar flow with constant physical properties and steady-state property, the governing equations are as follows.

– Continuity equation:

$$S_m = \frac{\partial \rho}{\partial t} + \frac{\partial}{\partial x_i}(\rho u_i) \tag{1}$$

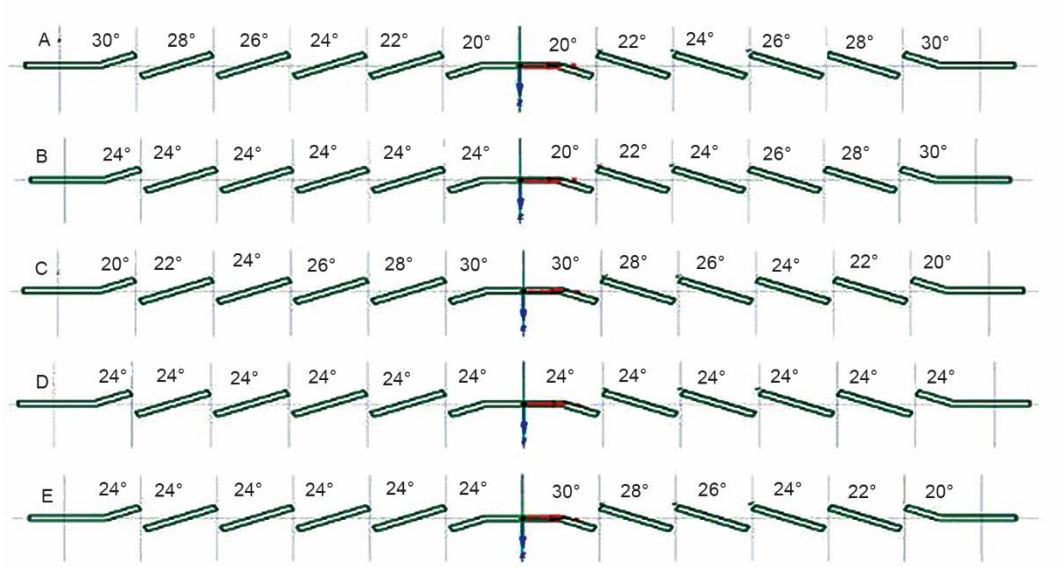

Figure 2. Structure of five kinds louver fins diagram

– Momentum conservation equation:

$$\frac{\partial}{\partial t}(\rho u_i) + \frac{\partial}{\partial x_j}(\rho u_i u_j) + \frac{\partial p}{\partial x_i} - \frac{\partial \tau_{ij}}{\partial x_j} = \rho g_i + F_i \tag{2}$$

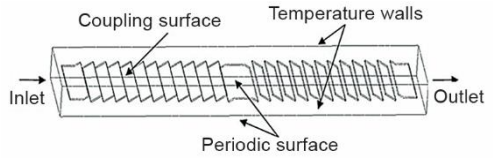

Figure 3. The 3-D structure of louver fins

– Energy equation:

$$S_h + \frac{\partial}{\partial x_i}\left[k_{\text{eff}} \frac{\partial T}{\partial x_i} - \sum_{j'} h_{j'} J_{j'} + u_j (\tau_{ij})_{\text{eff}} \right] = \frac{\partial}{\partial x_i}[u_i(\rho E + p)] + \frac{\partial}{\partial t}(\rho E) \tag{3}$$

where S_m is the source item, τ_{ij} – the stress tensor, p – the static pressure, F_i and ρg_i – the external volume force and gravitational volume force in the i direction, respectively, k_{eff} – the effective coefficient of heat conduction, $J_{j'}$ – the diffusion flux of component j', and S_h – the volumetric heat source term.

Data processing

In this paper, 3-D models of five fin structures are established and calculated by ANSYS17.1, the inlet pressure and outlet temperature of five groups of fin structures were calculated under the condition of inlet velocity 2.3 m/s and inlet temperature 293 K.

The results are treated by:

$$\mathrm{Re}_{LP} = \frac{\rho_a u d_e}{\mu} \tag{4}$$

$$h_{LP} = \frac{\dot{m} c_p (T_{out} - T_{in})}{A \Delta T_{LM}} \tag{5}$$

$$j = \frac{h}{\rho_a u c_p} \mathrm{Pr}^{2/3} \tag{6}$$

$$\Delta T_{LM} = \frac{(T_w - T_{out}) - (T_w - T_{in})}{\ln \dfrac{(T_w - T_{out})}{(T_w - T_{in})}} \tag{7}$$

$$\Delta p = P_{out} - P_{in} \tag{8}$$

$$f = 2 \frac{\Delta p}{\rho_a u^2} \frac{d_e}{L} \tag{9}$$

where ρ_a [kgm^{-3}] is the fluid density, u [ms^{-1}] – the fluid velocity, d_e [m] – the equivalent diameter of fin, μ [kgm^{-1}s^{-1}] – the coefficient of viscosity, h [Wm^{-2}K^{-1}] – the heat transfer coefficient, c_p [Jkg^{-1}K^{-1}] – the specific heat at constant pressure, T_{in} and T_{out} [K] – the fluid inlet and outlet temperatures, respectively, T_w [K] – the fin surface temperature, $\dot{m}$ [kgs^{-1}] – the mass-flow rate of fluid, $\mathrm{P_r} = 0.7$ – the Prandtl number, L [m] – the calculate length of the basin, and P_{in} and P_{out} [Pa] – the fluid inlet and outlet pressure, respectively.

Analysis of simulation results

Comparison of simulation results with empirical correlations

The example of fin E is given in this paper, the simulation results are compared with those of the empirical correlations fitted by Chang and Wang [14, 15], figs. 4-5 can be drawn out, and it can be seen that the results are basically the same, the simulation result of fin E is higher than that of empirical correlation. The errors of heat transfer coefficient and pressure drop are less than 10% and 15%, respectively, which are all within the error range, the results show that the numerical simulation and calculation method is correct.

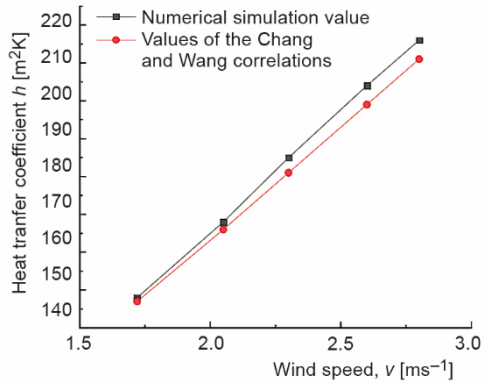

Figure 4. Comparison of heat transfer coefficient between simulated value and correlation value

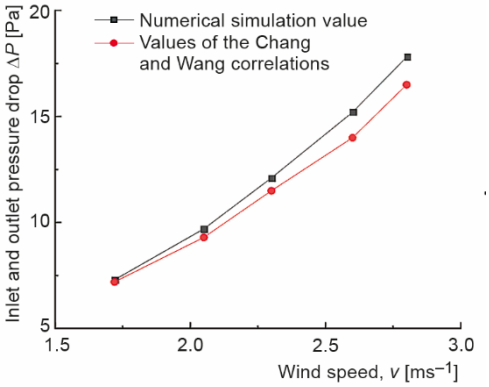

Figure 5. Comparison of import and export pressure drop between simulated value and correlation value

Analysis of simulation results of louver fins

In this paper, the initial temperature is 293 K and the wall temperature is 280 K, the model is kept unchanged, under the condition of u = 2.3 m/s and Re = 486.73, five kinds of fin structures were compared and analyzed, figs. 6-8 are the velocity field, temperature field and pressure field at the interface Y = 3.4 mm of five groups of fin models.

Figure 6 shows the velocity variation in the shutter at different angles. It can be seen that the velocity trend in the shutter is approximately the same. When the inclination of the shutter changes, the flow velocity in the channel changes accordingly. It can be seen directly from the diagram that the area of high-speed flow field in channel C and channel E is larger than that in channel D, and the area of high-speed flow field in model B is the largest, it can be shown that when the fin angle decreases from the middle to the left and right sides, the fluid disturbance can be enhanced and the high-speed flow field becomes larger.

Figure 7 shows the temperature variation of the five shutter angles. It can be seen that the exit temperature of the B structure is the lowest among the five groups of fin models. It is precisely because the high-speed flow field of the B structure in fig. 6 is the largest, the heat transfer on the fin surface is the most sufficient, the second is model C, and the outlet temperature of model A is the highest. The high temperature fluid flows from left to right, and the left part of the fin heat transfer more, as the fluid continues to flow, the temperature difference with the right part decreases, so the heat transfer effect decreases.

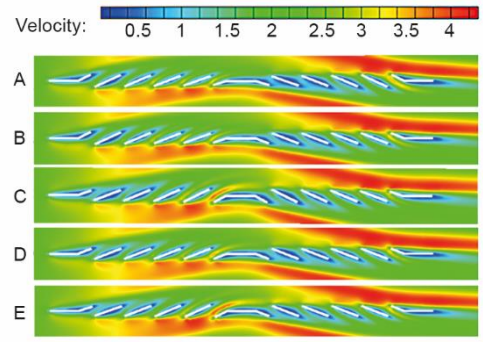

Figure 6. Contours of velocity at five louver angles

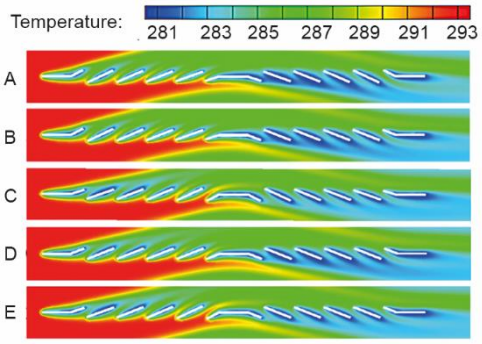

Figure 7. Contours of temperature at five louver angles

Figure 8 shows the contours of pressure of five fin models, in which the pressure drop at the fin structure C inlet is the largest, followed by that at the fin structure B, and the pressure drop at the exit of D structure and E structure is basically the same.

As can be seen from fig. 9, the heat transfer effect of B structure is the best among the five models, and the pressure drop of D model is the lowest. In the calculation, the heat transfer area, inlet velocity and initial temperature of the five fin structures are the same. The lower the liquid outlet temperature is, the better the heat transfer effect is. This result is consistent with the result of temperature field reaction in fig. 7. However, the heat transfer coefficient is not the only factor to measure the performance of the fin, but also needs to be evaluated with other indexes.

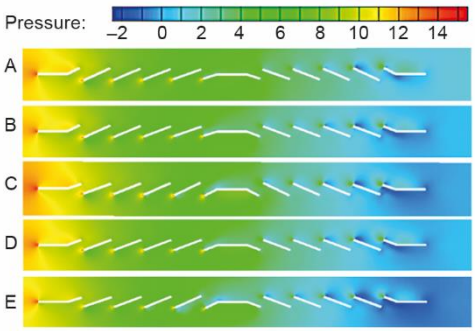

Figure 8. Contours of pressure of five louver angles

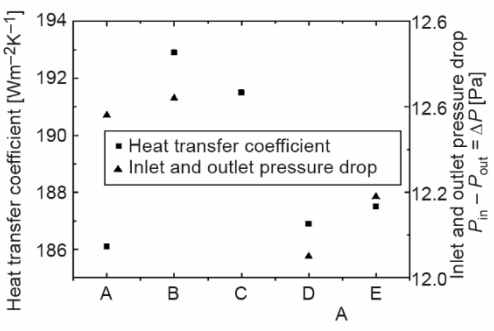

Figure 9. The diagram of heat transfer coefficient and pressure drop

Comprehensive performance evaluation of Louver fins with different angles

In order to compare the comprehensive performance of different shutter angles, the heat transfer performance and pressure drop of the fin model are analyzed and studied under the conditions of inlet wind speed of 1.7 m/s, 2.0 m/s, 2.3 m/s, 2.6 m/s, and 2.9 m/s.

Figure 10 shows that the heat transfer factor *j* for the B structure is always the highest at any speed in the five fin models. As the inlet velocity increases, the D structure and the E structure are gradually consistent, the heat transfer factor of A structure is minimized. As can be seen from fig. 11, the friction factor *f* of Model C is always the highest. When the velocity at the inlet is 2.9 m/s, the friction factor of model A and model B are basically the same, while that of Model D is always the lowest. When the velocity at the inlet of the channel increases, the decreasing trend of the five structures is approximately the same whether the friction factor *f* or the heat transfer factor *j*.

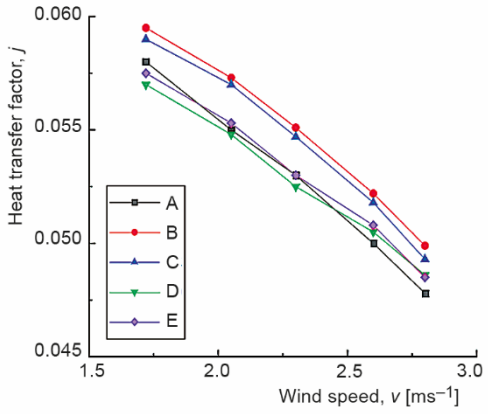

Figure 10. Effect of fluid velocity at the inlet on heat transfer factor

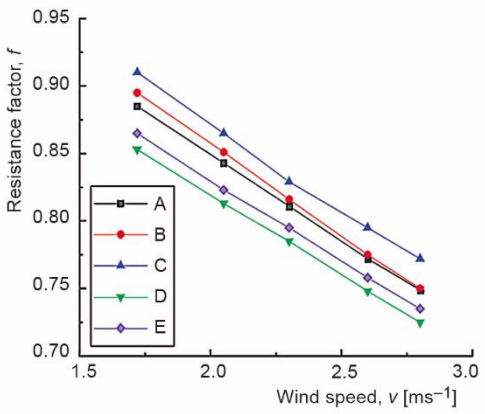

Figure 11. Effect of fluid velocity at the inlet *f* on resistance factor

By comparing the change trend of factor *j* and factor *f* of five fin structures, the heat transfer coefficient of B structure is the highest, followed by C structure, the pressure drop is

the highest, followed by B structure. In this paper, we adopt the method mentioned by Jiang and Zhai [16], that is, the bigger the j/f 1/3 ratio is, the better the comprehensive performance is, the comprehensive heat transfer effects of five fin models were compared. It can be seen from fig. 12 that the ratio of structure B is the highest and the comprehensive performance is the best no matter what the velocity at the entrance is. When the velocity at the inlet increases, the ratio of structure A becomes the smallest. Through analysis, the comprehensive performance of B structure is improved by 2.8~3.6% compared with A structure, by 1.1~1.5% compared with C structure, by 1.5~3.9% compared with D structure and by 2.2~2.9% compared with E structure.

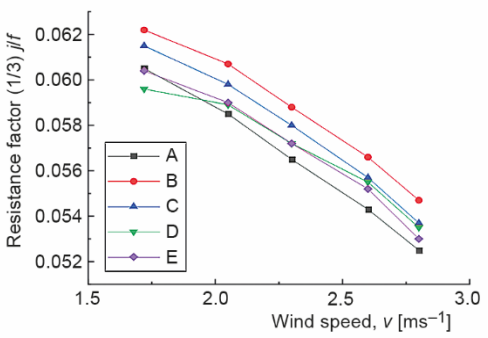

Figure 12. The $j/f^{1/3}$ of wind speed at different inlets

Discussion and conclusions

In this paper, the effects of different shutter angles on the heat transfer performance and pressure drop performance of parallel flow heat exchanger are studied by ANSYS17.1. The conclusions are as follows.

- The simulated values of heat transfer coefficient and pressure drop obtained in this paper are basically the same as those of the empirical correlations, and the errors of heat transfer coefficient and pressure drop are less than 10% and 15%, respectively, both within the allowable error range. That is to say, the calculation model and method adopted meet the requirements and are feasible.
- The velocity, temperature and pressure fields of five groups of fin structures were studied under the condition of 2.3 m/s wind velocity at the inlet. The study shows that the heat transfer coefficient of B structure is relatively the highest.
- By studying the comprehensive performance of five fin models with different angles, it is concluded that the model B presented in this paper has the best comprehensive performance compared with a uniform angle structure D and other three variable angle structures A, C, and E.
- Optimization of a parallel flow heat exchanger with heat transfer considerations should be carried out in a similar way as that in [17-20].

References

[1] Beamer, H. E., Cowell, T. A., Heat Exchanger Cooling Fin with Varying Louver Angle, United States Patent, 5730214, March 24, 1998
[2] Hsieh, C. T., Jang, J. Y., 3-D Thermal-Hydraulic Analysis for Louver Fin Heat Exchangers with Variable Louver Angle, *Applied Thermal Engineering, 26* (2006), 14-15, pp. 1629-1639
[3] Zhou, Y., *et al.*, Numerical Simulation of Heat Transfer And Drag Characteristics of Louver Fins (in chinese), *Power Engineering*, *25* (2005), Oct., pp. 191-194
[4] Zhou, Y., *et al.*, Three-Dimensional Numerical Simulation of Heat Transfer and Flow of Louver Fin (in chinese), *Energy Efficient Technologies*, *37* (2007) Sept., 102237
[5] Yan, L. L, Zhou, J. J., Three-Dimensional Numerical Simulation Of Air Side Flow and Heat Transfer in Louvered Fin-and-Tube Heat Exchanger (in Chinese), *Technology Communication*, *16* (2010), pp. 179-180

[6] Li, S. W., *et al.*, Study on the Influence of Louver Structure Parameters on the Flow and Heat Transfer Characteristics of Tube-Belt Radiator (in Chinese), *Internal Combustion Engines and Power Plants*, *87* (2022), Oct., 102230
[7] Guo, J. Z., *et al.,* The Analysis for Radiator Performance with Variable Angle Fin (in Chinese), *Modern Manufacturing Engineering*, (2019), 3, pp. 1-5
[8] Chen, C. L., *et al.*, Terminal Sliding Mode Control for Aeroelastic Systems, *Non-Linear Dynamics*, *70* (2012), 3, pp. 2015-2026
[9] Wang, C. C., *et al.*, Application of a Hybrid Numerical Method to the Bifurcation Analysis of a Rigid Rotor Supported by A Spherical Gas Journal Bearing System, *Non-linear Dynamics, 51* (2008), 4, pp. 515-528
[10] He, J. H., *et al.*, Insight into the Significance of Hall Current and Joule Heating on the Dynamics of Darcy-Forchheimer Peristaltic Flow of Rabinowitsch Fluid, *Journal of Mathematics, 2021* (2021), Oct., 3638807
[11] He, J. H., *et al.*, Improved Block-Pulse Functions for Numerical Solution of Mixed Volterra-Fredholm *Integral Equations, Axioms, 10* (2021), 3, 200
[12] Nadeem, G. A., *et al.*, New Optimal Fourth-Order Iterative Method Based on Linear Combination Technique, *Hacettepe Journal of Mathematics and Statistics*, *50* (2021), 6, pp. 1692-1708
[13] Khan, A., *et al.*, Numerical Approximation of Non-Linear Chromatographic Models Considering bi-Langmuir Isotherm, *Thermal Science*, *26* (2022), 1A, pp. 77-93
[14] Chang, Y. J, Wang, C. C., A Generalized Heat Transfer Correlation for Louver Fin Geometry, *Int. J. Heat Mass Transfer*, *40* (1997), 3, pp. 533-544
[15] Chang, Y. J., Wang, C. C., A Generalized Friction Correlation for Louver Fin Geometry, *International Journal of Heat and Mass Transfer*, *43* (2000), 12, pp. 2237-2243
[16] Jiang, L. X., Zhai, C., Numerical Simulation and Performance Analysis of Variable Angle Louver Fin, *Refrigeration Technology*, *40* (2012), 11, pp. 49-54
[17] Chen, C. L., *et al.*, Performance Analysis and Optimization of a Solar Powered Stirling Engine with Heat Transfer Considerations, *Energies*, *5* (2012), 9, pp. 3573-3585
[18] Vera-Rozo, J. R., *et al.*, Optimization of the Real Conversion Efficiency of Waste Cooking oil to FAME, *Thermal Science*, *26* (2022), 1B, pp. 653-665
[19] Shen, Y. Y., *et al.*, Subcarrier-Pairing-Based Resource Optimization for OFDM Wireless Powered Relay Transmissions with Time Switching Scheme, *IEEE Transactions on Signal Processing, 65* (2016), 5, pp. 1130-1145.
[20] Liu, X. Y., *et al.*, Optimization of a Fractal Electrode-Level Charge Transport Model, *Thermal Science*, *25* (2021), 3B, pp. 2213-2220

Paper submitted: August 23, 2021
Paper revised: July 16, 2022
Paper accepted: July 16, 2022